



*Citation for published version:*

Mattsson, T, Lewis, WJT, Chew, YMJ & Bird, MR 2015, 'In situ investigation of soft cake fouling layers using fluid dynamic gauging', *Food and Bioproducts Processing*, vol. 93, pp. 205-210.  
<https://doi.org/10.1016/j.fbp.2014.09.003>

*DOI:*

[10.1016/j.fbp.2014.09.003](https://doi.org/10.1016/j.fbp.2014.09.003)

*Publication date:*

2015

*Document Version*

Peer reviewed version

[Link to publication](#)

*Publisher Rights*

CC BY-NC-ND

**University of Bath**

**Alternative formats**

If you require this document in an alternative format, please contact:  
[openaccess@bath.ac.uk](mailto:openaccess@bath.ac.uk)

**General rights**

Copyright and moral rights for the publications made accessible in the public portal are retained by the authors and/or other copyright owners and it is a condition of accessing publications that users recognise and abide by the legal requirements associated with these rights.

**Take down policy**

If you believe that this document breaches copyright please contact us providing details, and we will remove access to the work immediately and investigate your claim.

# **IN SITU INVESTIGATION OF SOFT CAKE FOULING LAYERS USING FLUID DYNAMIC GAUGING**

Tuve Mattsson<sup>1,2</sup>, William J. T. Lewis<sup>3\*</sup>, Y.M. John Chew<sup>3</sup>, Michael R. Bird<sup>3</sup>

<sup>1</sup> Department of Chemical & Biological Engineering, Chalmers University of Technology, SE-412 96 Gothenburg, Sweden.

<sup>2</sup> Wallenberg Wood Science Center, The Royal Institute of Technology, Chalmers University of Technology, SE-100 44 Stockholm, Sweden.

<sup>3</sup> Department of Chemical Engineering, University of Bath, Claverton Down, Bath, BA2 7AY, UK

\*wjt20@bath.ac.uk

## **ABSTRACT**

*Cake fouling is a phenomenon contributing to flux decline during cross-flow filtration. Its behaviour is also difficult to predict, especially for challenging separations wherein organic materials often form compressible cakes with high resistance. In this study Kraft lignin was used as a model material for organic foulants in cross-flow microfiltration experiments, and a non-contact fluid dynamic gauging (FDG) technique in pressure-mode configuration was used to monitor the cake fouling layers in-situ. A novel and enhanced FDG equipment was used; enabling an increased accuracy of the fouling layer thickness measurements and capable of producing higher fluid shear stresses on the cake layer for strength measurements. Using FDG, very thin fouling layers were observed; in addition, FDG was used to investigate their cohesive and adhesive strengths, showing that over a 10-fold increase in fluid shear stress was required to remove foulant closer to the membrane compared with that on the surface of the cake.*

## **INTRODUCTION**

For solid-liquid separation, filtration is often the preferred method and is widely utilised in a range of industrial sectors. Advantages of filtration compared to other methods such as drying include a reduced energy consumption and a lower risk of thermal damage to the separated materials, which is of particular importance in food and beverage processing. Filtration can be run in several different modes; but membrane cross-flow filtration is particularly suitable for difficult-to-filter materials as the build-up of the high resistance filter cake on the membrane surface is counteracted by fluid shear imposed by cross-flow velocity (Belfort *et al.* 1994). Despite this, undesirable flux decline due to cake fouling is still one of the main issues in cross-flow filtration. Therefore fundamental understanding of cake fouling phenomena, especially for difficult-to-filter organic materials, is crucial for the design of efficient separation operations.

The effect of fouling during cross-flow filtration is readily apparent and is often investigated by measuring the flux decline under a constant transmembrane pressure (TMP), or alternatively, by examining increases in TMP under constant flux operation. For an

understanding of the underlying phenomena however, local properties need to be ascertained. One challenge presented in the investigation of cake fouling is the measurement of the height of the cake layer, which is preferably done *in situ* with limited disturbance to the layer. Chen *et al.* (2004) highlighted several existing non-invasive methods including Ultrasonic Time-Domain Reflectometry, Nuclear Magnetic Resonance, Laser Triangulometry and Direct Observation. A relatively new approach is Fluid Dynamic Gauging (FDG), which can estimate the thickness of cake layers during cross-flow filtration (Jones *et al.*, 2012), and can also be used in a destructive mode to estimate local strength properties throughout the different layers of the cake (Lewis *et al.*, 2012).

In this study, an enhanced FDG equipment is used to study soft cake fouling layers during cross-flow microfiltration of an organic model material, a Kraft lignin, which forms cohesive fouling layers and cakes which exhibit some degree of compressibility. Previous studies have concentrated on ultrafiltration under turbulent conditions (Jones *et al.*, 2012), or microfiltration of near ideal particle suspensions (Lister *et al.*, 2011). The use of lignin in this study demonstrates the complex behaviour of an organic material, which presents problems similar to those seen during the microfiltration of food based materials.

## EXPERIMENTAL

### *Material*

The model fouling material used in this study is a washed *Lignoboost*<sup>TM</sup> softwood Kraft lignin (Öhman *et al.*, 2008); an organic substance that forms cohesive fouling layers. *Lignoboost*<sup>TM</sup> lignin is a chemically modified lignin precipitated under acidic conditions from the black liquor in the Kraft process and contains different phenyl propane structural elements. As Kraft lignin is known to be alkali-soluble (e.g. Öhman *et al.*, 2007), the pH of the investigated suspensions was kept below 4 through addition of sulphuric acid to ensure that only precipitated lignin was present during experiments. The solid density of the lignin particles was measured at 1350 kg m<sup>-3</sup> using a gas pycnometer (AccuPyc II 1340, *Micromeritics*). The size distribution of the lignin suspension varied noticeably between experiments, and was characterised each time by laser diffraction (Mastersizer X, *Malvern*). Each experiment was performed with a total volume of 15 litres of 0.02 vol% suspension in reverse osmosis water at pH 3.7 (adjusted using sulphuric acid) at ambient temperature (16-19°C). The suspension was prepared right before each experiment from a stock slurry of 1-2 vol% lignin that had been stirred for at least 48 h to ensure sufficient dispersion.

The suspension was filtered using a hydrophilic regenerated cellulose membrane of 0.2 µm nominal pore size (RC58, *Whatman*), which was wetted prior to use. This pore size was selected so that all lignin particles were rejected by the membrane and cake formation was the predominant fouling mechanism.

### *Cross-flow filtration apparatus*

The basic technique of pressure-mode fluid dynamic gauging is explained fully elsewhere (Lewis *et al.* 2012). Thickness measurements are performed by measuring the pressure drop through a nozzle, shown in Figure 1 while a controlled flow of liquid,  $m_g$ , is drawn into it. The pressure drop is used to estimate the nozzle clearance,  $h$ . At a known clearance,  $h_0$ , from the surface the thickness reading,  $\delta$ , is calculated using  $\delta = h_0 - h$ . The apparatus used in this work was adapted and improved from that previously reported for cross-flow microfiltration by Lewis *et al.* (2012). Here, a smaller nozzle geometry (inner tube diameter,  $d = 3$  mm, nozzle opening diameter  $d_t = 0.5$  mm) was used, the dimensions of which are shown in Figure 1. This conferred the following advantages over its predecessor:

1. More accurate thickness measurements
2. Ability to study cake response to fluid shear stresses in excess of 50 Pa
3. Smaller footprint in the flow cell

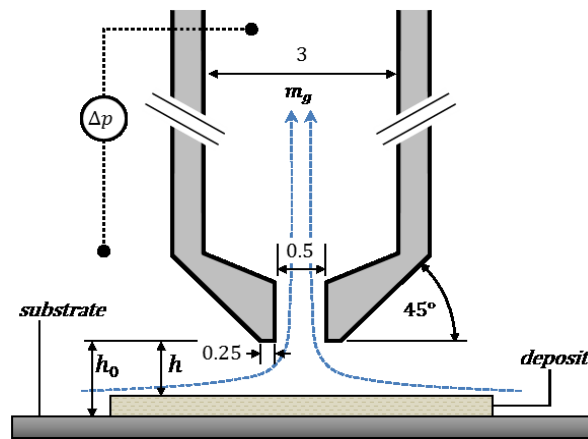


Figure 1. Schematic representation of the FDG nozzle, where  $\Delta p$  is used to indicate the clearance,  $h$  at an induced flowrate,  $m_g$ . Dimensions are in mm.

This nozzle was mounted on to a purpose-built polycarbonate test section, a schematic for which is shown in Figure 2. The test section housed a 250 mm flow channel of 15 mm square cross-section. A flat sheet membrane was mounted on to the bottom surface of this channel within a stainless steel cassette, which held it tightly against a porous spacer. The resulting flow cell within the test section contained a 150×15 mm porous surface set 1 mm lower than the rest of the flow cell, with tapered edges down to this point. The use of this setup allowed for facile removal of the membrane after experiments while avoiding loss of surface fouling. The bottom of the test section contained a small channel to collect permeate.

Thickness readings were determined by drawing fluid through the gauge using a syringe pump (Touchscreen 100 series, *Cole-Parmer*), whilst measuring pressure drop using a differential pressure transducer, dP1 (PX26-001DV, *Omega Engineering*). The gauge position was controlled from a PC by means of a stepper motor attached to a linear guide rail (KR1501AM, *THK*). The position was measured to an accuracy of  $\pm 0.5 \mu\text{m}$  by a linear variable differential transformer (SM-series LVDT, *RS Components*). The syringe pump was also connected to the PC, allowing fully remote control and automation of thickness readings.

Each thickness reading is also coupled with an indication of the fluid shear stress,  $\tau_w$ , imposed on the cake surface by gauging flows, which is a function of the gauge height,  $h$ . This is given by (Middleman 1998):

$$\tau_w = \mu \left( \frac{6m_g}{\rho h^2} \right) \frac{1}{d_t} \quad (1)$$

where  $\mu$  is the viscosity of the fluid,  $m_g$  is the mass flow of fluid through the gauge, and  $\rho$  is the density of the fluid. This value represents the greatest shear stress applied during FDG readings, which occurs at the inner edge of the nozzle rim (a radial distance of  $d_i/2$  from the centreline) (Chew *et al.*, 2004).

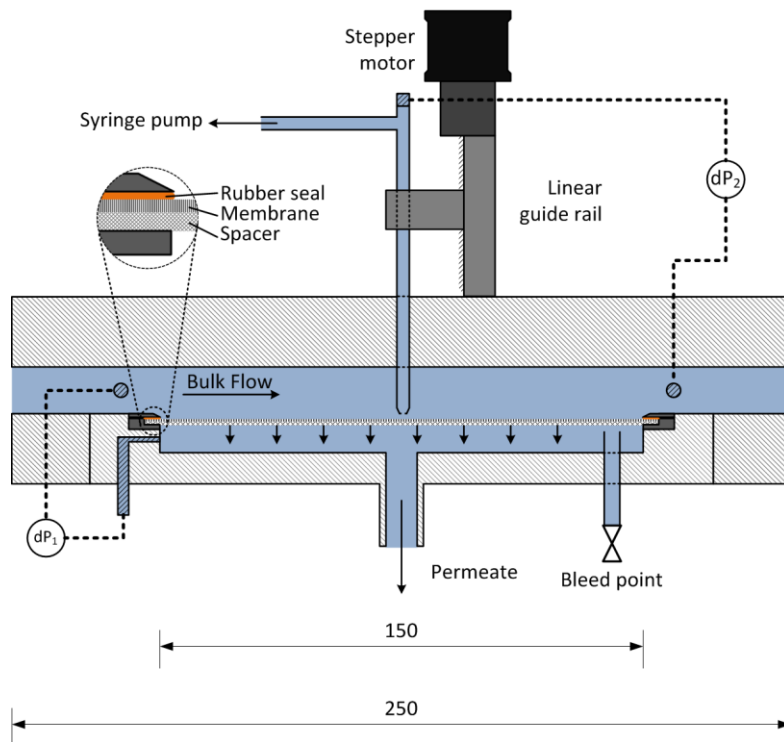


Figure 2. Schematic representation of polycarbonate test section. Dimensions are in mm. The two pressure transducers dP1 and dP2 are used for determination of TMP and for FDG measurements respectively.

The test section was mounted in the flow loop shown in Figure 3, which was operated in feed and bleed mode. Fluid was circulated from a feed tank through the test section by a centrifugal pump (P16, Charles Austen). A 500 mm entry section of 15 mm square duct was installed immediately prior to the test section to ensure laminar flow on entry. The cross-flow velocity was controlled using valves V2 and V5, and measured by a variable area flowmeter (1100-series Rotameter, KDG). Transmembrane pressure was controlled by a needle valve (V8) and measured by a differential pressure transducer, dP2 (PX26-005DV, Omega Engineering). Permeate was collected on an electronic balance (FX-3000i, A&D) which was connected to the PC for flow measurement.

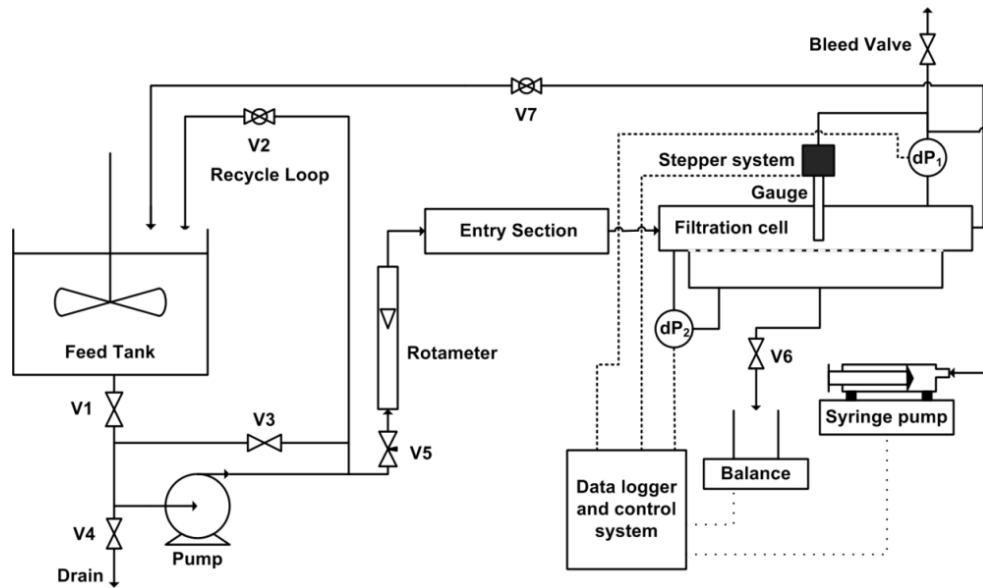


Figure 3. Schematic representation of the filtration rig.

### *Calibration for thickness measurements*

Thickness measurements were made by interpolating from a calibration plot of  $\Delta p$  vs.  $h/d_t$ . In previous work (Lewis *et al.* 2012) this plot had been determined by taking measurements over a clean stainless steel surface. For this apparatus, however, a plot was determined by computational fluid dynamics (CFD) simulations (not detailed in this work). This method was used because the position of the gauge at which  $h_0 = 0$  could not be set accurately enough against a solid surface.

An additional complication of performing FDG over membrane surfaces is that the position of the membrane can shift between experiments. In order to ensure the accuracy of thickness readings this must be taken into account. To correct for this, measurements of  $\Delta p$  vs.  $h/d_t$  over a clean membrane surface (where  $h = h_0$ ) were made in an automated sequence controlled by the PC. This included positioning of the gauge at various intervals of  $h/d_t$  and, with the syringe pump drawing fluid through the nozzle, taking a measurement of  $\Delta p$  for each. By inspection of this data when compared with the calibration plot, it was possible to identify the offset position of the membrane. This is demonstrated in Figure 4 wherein the same data is plotted against the CFD-derived calibration curve both before and after adjusting for offset. The entire process was built into the control system for this apparatus, allowing an offset to be adjusted prior to fouling experiments.

In this new setup, thickness readings with an accuracy of  $\pm 2.3 \mu\text{m}$  were achievable given an error in  $\Delta p$  of 0.25 mbar. At lower clearances, a resolution down to  $0.5 \mu\text{m}$  could be achieved, where it is limited by the accuracy of the LVDT. The automation of the calibration process and gauge movements greatly improved the speed at which experiments could be achieved compare with the earlier setup (Lewis *et al.* 2012). With further adaptations to the control program it should be possible to fully automate thickness measurements as well.

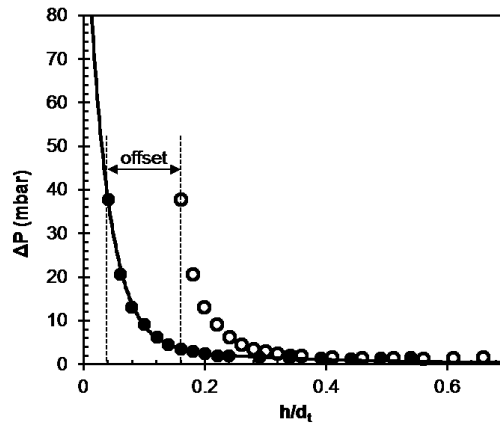


Figure 4. Calibration data profile for a membrane surface before (open symbols) and after (closed symbols) adjusting for offset. The solid line represents a calibration plot obtained from CFD.

### *Experimental conditions*

Filtration experiments were run in feed and bleed mode where no more than 0.9 L filtrate was withdrawn and the recovered cakes consisted of 1-3% of the total volume of lignin in the starting suspension. A TMP of 100 mbar was applied in all the experiments. The same cross-flow velocity ( $u = 0.1 \text{ m s}^{-1}$ ) was used in all of the experiments, corresponding to a Reynolds number,  $Re_{\text{duct}} = 1550$ . A fresh membrane was used in each experiment, and the position of the mounted membrane was calibrated using the gauge during a clean water filtration running at the set operating conditions. This procedure took about 10 min of which the automated calibration was completed within 3 min. After calibration, the filtration was commenced by adding 1 litre of diluted stock slurry directly to the feed tank. During the measurements of the cake layer, data was only collected while the gauge was at most  $h = 125 \mu\text{m}$  above the estimated position of the cake layer, as it is a principle of FDG that pressure changes become significant where  $h/d_t \leq 0.25$  (Tuladhar *et al.*, 2000). Thickness readings were made at the greatest clearance possible to reduce fluid shear stress on the surface of the cake which induces its removal.

Filtrations were commenced with the gauge retracted over 10 mm from the surface and no gauging flow active to avoid interference with cake growth. Because the stress imposed by the gauging flows on the cake during thickness measurements can cause some cake removal and/or impede its growth, successive thickness measurements were not taken during a single filtration. Instead each experiment was run up to a specific end-point time: 750, 1000, and 2000 s respectively, in order to attain a time-related estimation for cake growth. For each end-point time FDG was used to estimate cake thickness, then to perform destructive strength measurements by eroding the cake layer-by-layer. For each new strength measurement the probe was kept stationary until a stable value was recorded, the time required for the stabilisation, about 15 s, was similar at all positions with the exception of the very last measurements close to the membrane. The whole process took less than 400 s, with the thickness measurement completed within 100 s after the end-point time. Cross-flow filtration carried on during this process; however, due to the shear stress imposed by FDG on the cake surface, it is unlikely that further fouling in this position would occur.

## RESULTS & DISCUSSION

Between 6 and 7 experiments were performed for each end-point filtration time, from these experiments between 3 and 4 were deemed viable for further analysis based on their similar starting (clean water) flux, and concordance between the flux decline curves.

### *Characterisation*

Examples of particle size distributions of the lignin suspensions are shown in Figure 5, representing three cases: a low, medium and high average particle size. Characteristic values for the span are summarised in Table 1.

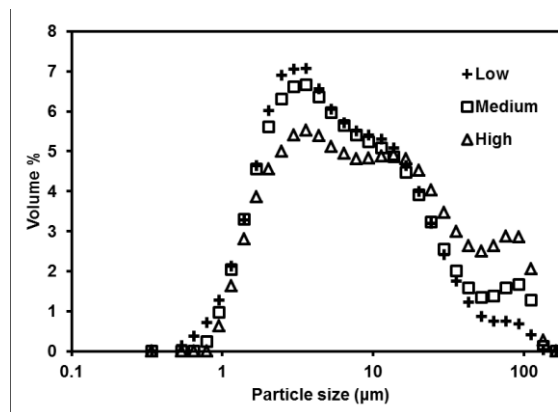


Figure 5. Size distribution of the lignin particles/agglomerates based on volume for three samples. The size distribution was measured using laser diffraction.

Table 1. Size distribution of the lignin particles/agglomerates from Figure 5.

$D_{(x)}$  indicates that  $x$  % in volume of the particles are smaller than the value stated, while  $D[3,2]$  denotes the surface area moment mean and  $D[4,3]$  the volume moment mean respectively.

	$D_{(10)}$ ( $\mu\text{m}$ )	$D_{(50)}$ ( $\mu\text{m}$ )	$D_{(90)}$ ( $\mu\text{m}$ )	$D[3,2]$	$D[4,3]$
Low	1.7	5.4	24.8	3.7	11.0
Medium	1.8	6.1	35.3	4.2	14.3
High	1.9	8.6	60.3	5.0	19.9

The difference between the size distributions are limited for the small particle range and much more pronounced for larger particles. These variations in particle size distributions were observed between different stock slurries and individual samples from the same slurry. Reasons for this have not yet been thoroughly explored but are likely to include small variations in their mechanical treatment (e.g. stirring); however these variations did not appear to have a significant impact on flux decline curves or the terminal flux. It **should** also be noted that even the smallest particles present were larger than the nominal membrane pore diameter of  $0.2 \mu\text{m}$ , indicating that the main fouling phenomenon should be surface/cake fouling.

### *Cross-flow filtration and cake layer characteristics*

Even for a suspension with such low lignin concentration as 0.02 vol%, a significant flux decline could be observed. Figure 6 shows that initial fouling on the surface had a high resistance, as indicated by the significant drop in flux at a constant TMP. The minor flux

increase that can be observed in the initial phase (Figure 6.b) can be contributed to a rise in TMP due to an increase in hydrostatic pressure upstream of the pump caused by the addition of lignin to the feed tank. The TMP needed to be manually regulated but was kept constant within  $\pm 5$  mbar during the whole experiment. Of the experiments deemed viable, as described above, the initial (clean water) flux was found to vary from 1720-1990  $\text{L m}^{-2} \text{h}^{-1}$ . These variations could be attributed to a small degree of background fouling, and small variations between temperature and available membrane area between experiments.

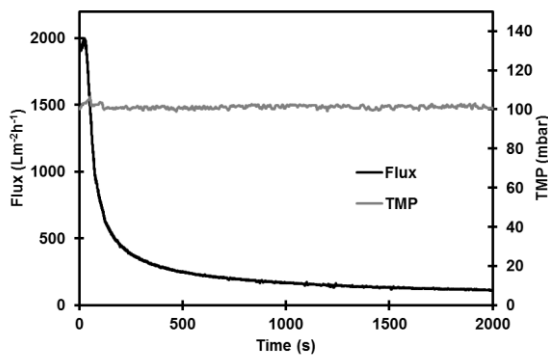


Figure 6.a. Flux decline and TMP during a 2000 s experiment.

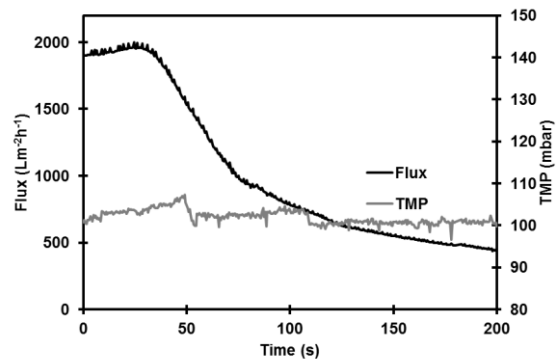


Figure 6.b. Initial flux decline and TMP during the first 200 s of a 2000 s experiment.

The viable flux decline curves for the three different end point times showed good agreement when superimposed, as demonstrated in Figure 7. Average cake thickness estimates and their spread are also shown in this figure. Some height measurements in the range  $0.2 < h/d_i \leq 0.25$  incurred an error larger than  $5 \mu\text{m}$  due to less stable pressure readings, these results were not considered in thickness estimates reported below. These unstable measurements could indicate the presence of a very loose layer on the top of the cake that is easily removed at low fluid shear stress.

A considerably high cake resistance was observed for relatively thin cake layers, and relating the estimated cake thickness to the particle size measured by laser diffraction indicates layers of 5-10 average particles or agglomerate diameters. The spread in the height estimates also tends to increase as the cake grows; an interesting phenomenon that could perhaps be related to deformation of the cake layer.

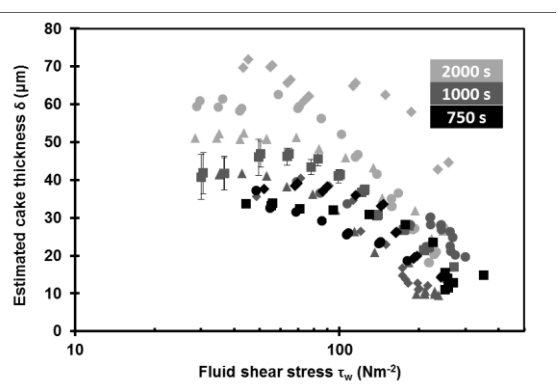
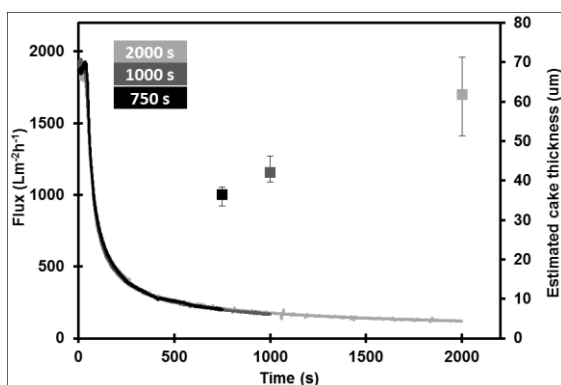


Figure 7. Example of flux decline curves from three different experiments (superimposed) together with average height measurements. Error bars indicates highest/lowest height estimate from the experiments.

Figure 8. Estimated cake thickness against calculated fluid shear stress for each filtration experiment. Note the log scale on the x-axis. Cake layers below 10  $\mu\text{m}$  could not be investigated due to high strength/proximity to the membrane.

Figure 8 shows the effect of the applied fluid shear stress from gauging flows on the cake thickness as the gauge is moved gradually towards the cake, removing the cake layers. The shear stress plotted is calculated from Eq. (1), which estimates the peak fluid shear on the surface below the gauge,  $\tau_w$ , which gives the maximum at a given clearance, occurring at the inner edge of the gauging nozzle (Lewis *et al.*, 2012). This gives an indication of the fluid shear stress required to remove the individual layers of the formed cake, i.e. an estimation of the local cohesive strength of the cake. These estimations also give an indication of the cross-flow conditions required for the removal of the individual cake layers. The figure shows how the strength of the cake layers increase 10-fold as the membrane is approached (note the log scale on the x-axis). This indicates that the removal of the cake fouling layer closest to the membrane is difficult to achieve. Further studies of the effects of varying TMP are underway, and cake thickness readings are used with gravimetric analyses to indicate cake solidosity and specific resistance.

## CONCLUSIONS

The cake fouling for cross-flow microfiltration of a model material, Kraft lignin, was investigated with fluid dynamic gauging. The new smaller gauge (with a nozzle throat diameter of  $d_t = 0.5$  mm) could be used to successfully indicate the growth of the cake, as well as for estimations of local cohesive cake strength throughout the cake, down to 10-20  $\mu\text{m}$  from the membrane. Combined flux measurements and thickness estimates indicate a high-resistance fouling layer less than 100  $\mu\text{m}$  thick developed within less than an hour's filtration time. Strength measurements indicate a 10-fold increase in cohesive strength of the local cake layers when comparing the layers close to the membrane with the top layers.

## ACKNOWLEDGEMENTS

The financial support for this work by the Knut and Alice Wallenberg Foundation and Chalmers energy initiative is gratefully acknowledged. Financial support at the University of Bath was provided by the EPSRC.

## NOMENCLATURE

*Roman*

$d$	inside diameter of gauge tube [m]
$d_t$	inside diameter of nozzle throat [m]
$h$	gauge height above a deposit [m]
$h_0$	gauge height above the membrane [m]
$m_g$	mass flow of fluid through the gauge [ $\text{kg s}^{-1}$ ]

$u$  cross flow velocity in the test section [ $\text{m s}^{-1}$ ]  
 $\Delta p$  pressure drop [Pa]

#### *Greek*

$\delta$  filter cake thickness [m]  
 $\mu$  viscosity of the fluid [Pa s]  
 $\rho$  density [ $\text{kg m}^{-3}$ ]  
 $\tau_w$  fluid shear stress [ $\text{N m}^{-2}$ ]

#### *Acronyms*

dP Differential pressure  
FDG Fluid Dynamic Gauging  
LVDT Linear Variable Differential Transformer  
TMP Transmembrane Pressure

#### REFERENCES

- Belfort, G., Davis, R.H. and Zydney, A.L., (1994) - The behavior of suspensions and macromolecular solutions in crossflow microfiltration. *J Membrane Sci*, 96:1-58.
- Chen, V., Li, H. and Fane, A. G. (2004) - Non-invasive observation of synthetic membrane processes - a review of methods. *J Membrane Sci*, 241: 23-44.
- Jones, S. A., Chew, Y. M. J., Wilson, D. I. and Bird, M. R., (2012) - Fluid dynamic gauging of microfiltration membranes fouled with sugar beet molasses. *J Food Eng*, 108: 22-29.
- Lewis, W. J. T., Chew, Y. M. J. and Bird, M. R., (2012) - The application of fluid dynamic gauging in characterising cake deposition during the cross- flow microfiltration of a yeast suspension. *J Membrane Sci*, 405-406: 113-122.
- Lister, V.Y., Lucas, C., Gordon, P.W., Chew, Y.M.J. & Wilson, D.I. (2011) - Pressure mode fluid dynamic gauging for studying cake build-up in cross-flow microfiltration, *J Membrane Sci*, 366: 304-313.
- Middleman, S. 1998, An introduction to fluid dynamics: principles of analysis and design, (Wiley, Chichester, New York, USA)
- Öhman, F., Theliander, H., Tomani, P. and Axegård, P., (2008) - Method for separating lignin from black liquor, US-patent 2008/0047674.
- Öhman, F., Wallmo H. and Theliander, H., (2007) - A novel method for washing lignin precipitated from kraft black liquor – Laboratory trials. *Nord. Pulp Paper Res*, Vol 22 (1): 9-16.
- Tuladhar, T. R., Paterson, W. R., Macleod, N. and Wilson, D. I. (2000) - Development of a novel non-contact proximity gauge for thickness measurement of soft deposits and its application in fouling studies. *Can J Chem Eng*, 78: 935-947.